Compression of Single Conjugated-polymer Nanoparticles with AFM Tips

Xingfei Zhou,[†,†††] Hui Xu,[†] Chunhai Fan,*[†] Jielin Sun,[††] Yi Zhang,[†] Minqian Li,[†] Wenqing Shen,[†] and Jun Hu*[†,††]
[†]*Shanghai Institute of Applied Physics, Chinese Academy of Sciences, Shanghai 201800, P. R. China*
[††]*Bio-X Life Science Research Center, Shanghai Jiao Tong University, Shanghai 200030, P. R. China*
[†††]*Nanomaterials Laboratory, College of Sciences, Ningbo University, Ningbo 315211, P. R. China*

(Received June 13, 2005; CL-050760)

A water-soluble conjugated polymer, poly[lithium 5-methoxy-2-(4-sulfobutoxy)-1,4-phenylenevinylene] (MBL-PPV), spontaneously forms nanoparticles at flat mica surfaces. In this work, we manipulated single PPV nanoparticles with a modified version of AFM, our recently developed vibrating scanning polarization force microscopy (VSPFM). VSPFM provides a new way to obtain undistorted imaging of "soft" molecules at surfaces. We have demonstrated that we could stepwise compress a single PPV nanoparticle with an AFM tip and estimate its compression elasticity in a small force regime.

Poly(*p*-phenylenevinylene) (PPV) is a kind of typical conjugated polymer,[1] which represents a new class of functionalized materials possessing a unique combination of optoelectronic properties.[2,3] Previous studies have demonstrated that deposition of short PPV chain on solid surface leads to the formation of a variety of nanostructures such as nanoparticle, nanorod, and nanoribbon, depending on the properties of PPV derivatives and experimental conditions.[4] It is of great significance to manipulate these nanostructures for in-depth understanding of mechanical properties of conjugated materials that might ultimately contribute to the design of electromechanical and photonic nanodevices.[5] We recently developed vibrating scanning polarization force microscopy (VSPFM), a unique technique that opens an avenue to obtain undistorted imaging of "soft" molecules as well as elastic properties of soft materials at nanometer scale.[6,7] With VSPFM we have reliably measured the height of biomolecules deposited on mica surface.[7] Herein, we report the compression of a single PPV nanoparticle with this new technique.

The polymer employed in this study is an negatively charged, water-soluble conjugated polyelectrolyte, poly[lithium 5-methoxy-2-(4-sulfobutoxy)-1,4-phenylenevinylene] (MBL-PPV).[8] A droplet of diluted MBL-PPV solution (ca. 5 μL) was placed on freshly cleaved mica surface and then extensively washed with Millipore water (18.2 MΩ). Finally, the sample was dried under a gentle steam of air.

VSPFM is a modified version of NanoScope IIIa SPM system (Veeco Instruments, Inc., Santa Barbara, CA) as described in Ref. 7. Briefly, in VSPFM an ac voltage (ca. 6–10 V) is applied between the tip and sample, thus a polarization electrostatic field is established. The electrostatic force is used as trace force before the biased-tip touches the sample surface, after the tip touches the sample the repulsive force dominates the tip/sample interaction.[7] Since the range of electrostatic force (ca. 10 nm) is much longer than that of van der Waals attractive force (ca. 1–2 nm), VSPFM can be performed in far non-contact, near non-contact, and tapping regions by carefully adjusting the value of amplitude setpoint (Asp). The absolute value of tip vibration amplitude can be extracted from amplitude–distance curve.

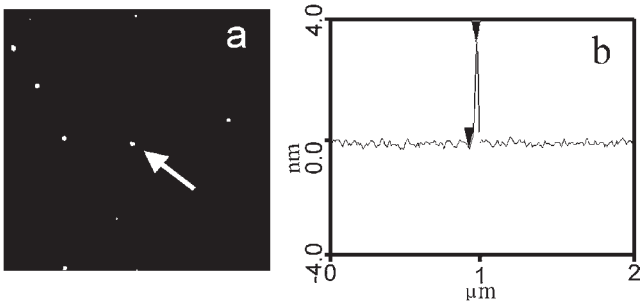

Figure 1. (a) The topography (height) of PPV nanoparticles deposited on mica surface in air, Image size: $2 \times 2\,\mu m^2$. (b) The height profile of one nanoparticle as indicated in (a).

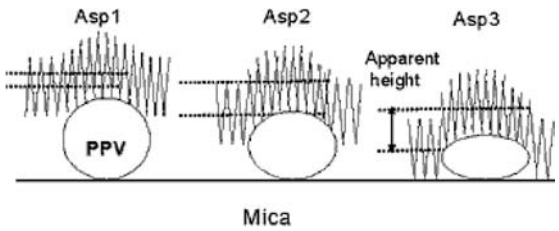

Figure 2. Sketch of a PPV nanoparticle tethered to a mica surface and an AFM tip at three different set point values (Asp1 > Asp2 > Asp3). The scanning tip only imaged the PPV particle and did not image the mica surface (Asp1 and Aps2).

In our experiment, we employed a conductive NSC12/Pt rectangular cantilever (MicroMasch) with a spring constant of ca. 4.5 N/m and a resonant frequency of ca. 170 kHz. The images were taken at the temperature of 25–30 °C under the relative humidity of 20–30%.

We observed that MBL-PPV automatically forms nanoparticles at a freshly cleaved mica surfaces under our experimental conditions. Figure 1a shows a typical high-resolution topographical image of PPV nanoparticles. The average apparent height and the width of these nanoparticles are about 3.8 and 30 nm (Figure 1b), respectively. These values are reasonable for nanoparticles, taking into consideration of the tip convolution effect. To begin the compression we selected a well-shaped particle as a target. First Asp was increased gradually until the contrast of PPV particles disappeared in the image. In this case, the tip did not touch the top of molecule. With the decrease of Asp, the tip was then located to scan on the top of the molecule at a large Asp and lowered step by step until a conventional tapping-mode AFM (TM-AFM) images appeared, as shown in Figure 2. The corresponding Asp was written as Asp_{top} and Asp_{bottom}, respectively. Thus a series of images could be taken during this approach. It is worth to stress that the position of the tip can be precisely controlled with the accuracy about 0.1 nm and images can be taken at each position by finely tuning Asp of

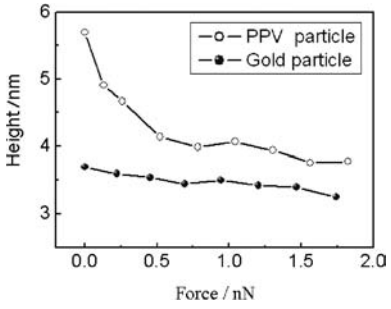

Figure 3. Height–force curves for the PPV nanoparticle and gold particle.

our VSPFM. The height D_j of PPV nanoparticles after compressing j-th step can be calculated according to the following Eq 1:

$$D_j = D_{j\text{-app}} + \alpha \times (\text{Asp}_j - \text{Asp}_{\text{bottom}}), \quad (1)$$

where Asp_j is the vibration amplitude; $D_{j\text{-app}}$ denotes apparent height of nanoparticles and can be determined from the offline treatment; α is a conversion coefficient, which is defined as: in a zero-scale scan on mica surface, we can change the set-point value Asp stepwise. A given change ΔAsp would induce a stepwise change ΔZ in the tip-sample distance, which can be directly measured from the offline topographic image.

A single PPV nanoparticle on mica surface was compressed with an AFM tip as described above. Importantly, we can record the deformation of a PPV particle during the compression process, and concurrently monitor this process right from the point that the tip slightly touched the top of the particle to the point that the particle was severely compressed (Supporting Information). The deformation of particle was calculated in terms of Eq 1 according to the corresponding Asp. The force on the nanoparticle was calibrated by a soft cantilever with known spring constant.[9]

Figure 3 is a typical height–force plot that represents the compressing process of a PPV nanoparticle. It illustrates that the compression of a PPV nanoparticle is nonlinear. In the initial compressing stage (<0.5 nN), the height decreases rapidly with the applied force, suggesting that PPV nanoparticles are "soft" and susceptible to even small forces. As a comparison, the well known "hard" gold nanoparticles exhibit a fairly flat height–force curve, which means that its height does not significantly change with the increase of applied forces (Figure 3). When the average load is beyond 0.5 nN, the height–force curve of PPV nanoparticles becomes flat. At this stage, the PPV nanoparticles has been so compressed that the tip is encountered with strong repulsive force, thus the normal force rapidly increases with little further compression. The compression elasticity of PPV nanoparticles can be extracted from the slope of the height–force curve in the small force regime with Hertz model, which is widely used to estimate the elastic modulus of single nanoparticle in AFM experiment. We note that the elastic moduli of tip and substrate (mica) are significantly higher than that of PPV nanoparticles, thus the deformation of the tip and substrate are negligible. According to this, the Hertz model is simplified to the following equation[10]

$$d^3 = 9(1 - v)^2 {F_0}^2/(16RE^2), \quad (2)$$

where v, R, F_0, d, and E represent the Posisson ration, tip radial, applied load, indentation, and Young's modulus, respectively. The tip radial R is ca. 20 nm, as provided by the manufacturer. By assuming a typical Posisson ration is 1/3 for soft materials, and fitting the functional dependence of Eq 2 to several height–force curves, we obtained the effective elastic modulus of PPV nanoparticles: 14 ± 6 Mpa. This value is reasonably lower than that obtained from mechanical spectroscopy of PPF film (ca. 50 Mpa).[11] It is likely due to the different PPV derivatives, and more importantly, the PPV states in the film and on the surface (more lateral constraints are expected for PPV in films state than PPV free on surfaces). We note that the PPV compression can be reversed by removing the applied force, suggesting that the deformation of PPV is elastic. It is also worthwhile to point out that the applied compression force should significantly influence optical properties of PPV. This relationship might be probed by combining VSPFM and single-molecule spectroscopy.

We also note that the height of the PPV nanoparticles is approx. 5.7 nm before the initial compression. This value is markedly larger than that obtained with TM-AFM (ca. 3.8 nm). This difference suggests that the tip pressure is one of the key factors that result in polymer deformation. As a fact, the effect of tip pressure has been gradually realized and suggested to take into account in AFM imaging of "soft" molecules. For example, a recent AFM imaging study on a IgG protein molecule indicated that its severe deformation was induced by AFM tip pressure.[12] While the conventional TM-AFM unavoidably images molecules at certain applied forces, our VSPFM-based method can study molecules when the tip/molecule interaction approaches zero, which offers new opportunities for investigation of "soft" materials.

In conclusion, we have demonstrated that based on our newly developed VSPFM technique we can stepwise compress a single PPV nanoparticle with an AFM tip and estimate its compression elasticity. In fact, our VSPFM-based method is not limited to the elastic measurement, other applications such as conductivity images, water film mapping are also under way in our laboratory.

The authors gratefully thank the financial support of the projects by National Natural Science Foundation (Nos. 20404016 and 10304011), Shanghai Rising-Star Program, Ministry of Science and Technology of China (No. 2003AA226011), Shanghai Municipal Commission for Science and Technology (Nos. 0452nm068 and 03DZ14025), and Chinese Academy of Sciences.

References

1 L. H. Chen, D. W. McBranch, H. L. Wang, R. Helgeson, F. Wudl, and D. G. Whitten, *Proc. Natl. Acad. Sci. U.S.A.*, **96**, 12287 (1999); C. Fan, K. W. Plaxco, and A. J. Heeger, *J. Am. Chem. Soc.*, **124**, 5642 (2002); C. Fan, S. Wang, J. W. Hong, G. C. Bazan, K. W. Plaxco, and A. J. Heeger, *Proc. Natl. Acad. Sci. U.S.A.*, **100**, 6297 (2003).
2 F. Hide, M. A. Diaz-Garcia, B. J. Schwartz, M. R. Andersson, Q. Pei, and A. J. Heeger, *Science*, **273**, 1833 (1996); J. Pei, W. Yu, W. Huang, and A. J. Heeger, *Chem. Lett.*, **1999**, 1123; M. T. Bernius, M. Inbasekaran, J. O'Brien, and W. Wu, *Adv. Mater.*, **12**, 1737 (2000).
3 R. H. Friend, R. W. Gymer, A. B. Holmes, J. H. Burroughes, R. N. Marks, C. Taliani, D. D. C. Bradley, D. A. Dos Santos, J. L. Bedas, M. Logdlund, and W. R. Salaneck, *Nature*, **397**, 121 (1999).
4 Y. Luo, H. Liu, F. Xi, L. Li, X. Jin, C. Han, and C. Chan, *J. Am. Chem. Soc.*, **125**, 6447 (2003).
5 J. Kim and T. M. Swager, *Nature*, **411**, 1030 (2001); J. Yu, D. Hu, and P. F. Barbara, *Science*, **289**, 1327 (2000); H. G. Graighead, *Science*, **290**, 1532 (2000).
6 J. Hu, X. Xiao, and M. Salmeron, *Science*, **268**, 267 (1995).
7 X. Li, J. Sun, X. Zhou, G. Li, P. He, Y. Fang, M. Li, and J. Hu, *J. Vac. Sci. Technol., B*, **21**, 1070 (2003); X. F. Zhou, J. L. Sun, H. J. An, and J. Hu, *Phys. Rev. E*, **71**, 062901 (2005).
8 D. Wang, Ph.D. Dissertation, University of California, Santa Barbara (2001).
9 C. Su, L. Huang, and K. Kjoller, *Ultramicroscopy*, **100**, 233 (2004).
10 M. Radmacher, M. Fritz, J. P. Cleveland, D. A. Walters, and P. K. Hansma, *Langmuir*, **10**, 3809 (1994).
11 A. Nagy, A. Strahl, H. Neuhauser, S. Schrader, I. Behrens, E. Peiner, and A. Schlachetzki, *Mater. Sci. Eng., A*, **370**, 311 (2004).
12 R. Garcia and R. Perez, *Surf. Sci. Rep.*, **47**, 197 (2002).

Published on the web (Advance View) September 28, 2005; DOI 10.1246/cl.2005.1488